JOURNAL OF GEOPHYSICAL RESEARCH, VOL. 114, D13203, doi:10.1029/2009JD011772, 2009

Subarctic atmospheric aerosol composition: 1. Ambient aerosol characterization

Beth Friedman,[1,2] Hanna Herich,[3] Lukas Kammermann,[4] Deborah S. Gross,[2] Almut Arneth,[5] Thomas Holst,[5] and Daniel J. Cziczo[3,6]

Received 20 January 2009; revised 12 April 2009; accepted 16 April 2009; published 10 July 2009.

[1] Subarctic aerosol was sampled during July 2007 at the Abisko Research Station Stordalen field site operated by the Royal Swedish Academy of Sciences. Located in northern Sweden at 68° latitude and 385 m above sea level (m asl), this site is classified as a semicontinuous permafrost mire. Number density, size distribution, cloud condensation nucleus properties, and chemical composition of the ambient aerosol were determined. Back trajectories showed that three distinct air masses were present over Stordalen during the sampling period. Aerosol properties changed and correlated with air mass origin to the south, northeast, or west, suggesting that particle source and transport were important factors. We observe that Arctic aerosol is not compositionally unlike that found in the free troposphere at midlatitudes. Internal mixtures of sulfates and organics, many on insoluble biomass burning and/or elemental carbon cores, dominate the number density of particles from ~200- to 2000-nm aerodynamic diameter. Mineral dust that had interacted with gas-phase species was observed in all air masses. Sea salt, due to the uptake of nitrate species and loss of chlorine, was the aerosol type that most varied chemically with air mass.

Citation: Friedman, B., H. Herich, L. Kammermann, D. S. Gross, A. Arneth, T. Holst, and D. J. Cziczo (2009), Subarctic atmospheric aerosol composition: 1. Ambient aerosol characterization, *J. Geophys. Res.*, *114*, D13203, doi:10.1029/2009JD011772.

1. Introduction

[2] Aerosol particles can affect their environment in multiple ways. The Earth's radiative balance is one example and it is affected by several distinct mechanisms. Aerosols can scatter and absorb solar radiation (the direct aerosol effect) [*McCormick and Ludwig*, 1967; *Coakley et al.*, 1983]. Aerosols act as cloud condensation nuclei (CCN) or ice nuclei, leading to cloud formation and/or alteration of microphysical and radiative properties (the indirect aerosol effect) [*Twomey*, 1977; *Albrecht*, 1989; *Lohmann and Feichter*, 2005]. Aerosols can also absorb radiation from within clouds, thereby perturbing their temperature profile and stability (the semidirect effect). Because of the complex interaction of aerosols, clouds and climate this area represents one of the major uncertainties in our current understanding of climate change [*IPCC*, 2007].

[3] Individual aerosol particles are typically internal mixtures of a variety of chemical compounds [e.g., *Murphy and Thomson*, 1997a, 1997b]. In addition to its size [*Dusek et al.*, 2006] the chemical composition of an aerosol particle determines whether it has the ability to take up water and act as a CCN [*Baltensperger et al.*, 2002; *Hegg et al.*, 2006]. Aerosol composition and water content also determine the optical and chemical properties of the particle. Aerosols consisting of light-absorbing materials such as soot absorb sunlight directly and have a warming effect whereas sulfates predominantly scatter and cool [*Penner et al.*, 1998; *Bond and Bergstrom*, 2006]. Reactions, for example the hydrolysis of N_2O_5, have also been shown to be dependent on the composition-related water content of the particle [*Hu and Abbatt*, 1997]. A knowledge of aerosol size and mixing state are thus critical components for a better understanding of atmospheric chemistry and climate change.

[4] Climate change has been more pronounced in the Arctic region than elsewhere, with a temperature increase twice that of the global average [*IPCC*, 2007]. It has largely been assumed that direct aerosol effects at Arctic latitudes are small owing to the low solar elevation. However, the surface albedo in polar regions is often high owing to snow and ice cover and this can lead to multiple reflections if absorbing particles are suspended above such surfaces [*Chýlek and Coakley*, 1974; *Randles et al.*, 2004]. There is also a relatively larger uncertainty at high latitudes because there is less atmospheric field data owing to difficult access conditions and often severe temperatures and weather. The lack of field data has resulted in limited

[1]Department of Atmospheric Sciences, University of Washington, Seattle, Washington, USA.
[2]Department of Chemistry, Carleton College, Northfield, Minnesota, USA.
[3]Institute for Atmospheric and Climate Science, ETH Zurich, Zurich, Switzerland.
[4]Laboratory of Atmospheric Chemistry, Paul Scherrer Institut, Villigen, Switzerland.
[5]Department of Physical Geography and Ecosystems Analysis, Lund University, Lund, Sweden.
[6]Now at Atmospheric Science and Global Change, Pacific Northwest National Laboratory, Richland, Washington, USA.

0148-0227/09/2009JD011772$09.00

information about how the Arctic is influenced by continental pollutants, the chemical composition and transport processes of aerosols, and the relationship between particles and clouds. Increasing our understanding of Arctic regional climate change and acquiring high-quality atmospheric data are two of the objectives of the most recent International Polar Year (A Framework for the International Polar Year 2007–2008 produced by the ICSU IPY 2007–2008 Planning Group, 2004, International Council for Science, available at http://www.ipy.org).

[5] Although there are relatively few anthropogenic pollution sources in the Arctic, this region is known to be impacted by emissions from lower latitudes. For example, in late winter and spring the Arctic is affected by a so-called "Arctic Haze" consisting of pollutants mainly from Europe and Asia [*Mitchell*, 1957; *Heintzenberg*, 1980]. In late spring and summer, plumes from boreal forest fires can be carried to the Arctic [e.g., *Dibb et al.*, 1996]. Besides the Arctic Haze phenomenon, measurements in Arctic and subarctic regions have also focused on nucleation events [*Kulmala et al.*, 2001] which occur predominantly during spring and autumn over boreal forest regions (summarized by *Kulmala et al.* [2004]). At one high-latitude location the peak number of new particle formation, in some cases with very high growth rates, was observed during summer [*Svenningsson et al.*, 2008]. Several properties of these biogenic particles have been further investigated. *Lihavainen et al.* [2003] concentrated on the CCN production resulting from new-particle formation, and *Komppula et al.* [2005] evaluated size-resolved cloud droplet number concentrations in subarctic Finland. The boreal forest particle studies concentrated mainly on nucleation and Aitken mode particles. A commercial Aerodyne aerosol mass spectrometer (AMS) was used to study the aerosol composition in instances of high densities of recently formed particles, finding that they had a predominantly organic composition [*Allan et al.*, 2006]. The same type of instrument was also used to resolve the composition of cloud droplet residuals [*Drewnick et al.*, 2007].

[6] In this study an aerosol time-of-flight mass spectrometer (ATOFMS) [*Gard et al.*, 1997], commercially available from TSI (Model 3800, TSI Inc., Minnesota), was operated at the Abisko Research Station Stordalen field site. SPMS has been deployed in various field studies [e.g., *Sullivan and Prather*, 2005] but never before, to our knowledge, at Arctic latitudes. As such this work complements the aforementioned studies.

2. Experimental Methods

2.1. Overview

[7] The purpose of this study was to characterize the ambient conditions and aerosol properties in a remote Arctic region unaffected by significant local anthropogenic particle sources or precursors. Our foremost goal is to compare and contrast particle properties (i.e., size, number, and chemical composition) as a function of air mass origin in this region. A secondary objective is to provide an overview of the instrumentation, sampling location, methodology, and meteorology for this and companion publications.

[8] Single particle mass spectroscopy (SPMS) is a tool for determining the size, chemical composition and mixing state on a particle by particle basis both in situ and in real time. This is unlike previously studies of Arctic aerosol which have been restricted to bulk samples and emission inventories [*Quinn et al.*, 2008, and references therein]. Studies with an AMS average over a mass-dependent group of particles and resolve only volatile and semivolatile components; substances such as sea salt, elemental carbon, and mineral dust cannot be observed [*Allan et al.*, 2006; *Drewnick et al.*, 2007]. Previous studies at the single particle level have been carried out on collected samples returned to a laboratory for in vacuo studies with electron microscopy which results in volatile material loss and extensive preparation and analysis time [*Niemi et al.*, 2006; *Behrenfeldt et al.*, 2008]. In this study an ATOFMS was operated in conjunction with other instruments near Abisko, Sweden during the month of July 2007. Multiple measurement strategies were employed. The ATOFMS sampled for long periods from three distinct air masses originating from different directions, each of which had different particle characteristics. The ATOFMS was periodically connected to a hygroscopicity tandem differential mobility analyzer (HTDMA) to measure the aerosol chemical composition as a function of the hygroscopic growth. This data is discussed in a companion paper [*Herich et al.*, 2009]. Besides the ATOFMS and the HTDMA, a scanning mobility particle sizer (SMPS) was used to determine submicrometer mobility diameter particle number density, a condensation particle counter (CPC) was used to determine total aerosol number, and a CCN counter (CCNC) was used to determine the number density of cloud forming aerosol as a function of supersaturation. Data from the CCN and HTDMA, when the latter was not connected to the ATOFMS, are discussed in a second companion paper (L. Kammermann et al., Subarctic atmospheric aerosol composition: 3. Measured and modeled properties of cloud condensation nuclei, manuscript in preparation, 2009). Meteorological factors such as wind speed, wind direction, and temperature were also monitored. Finally, back trajectories were determined to differentiate and characterize the air masses.

2.2. Sampling Site

[9] Stordalen mire (68°22′N 19°03′E) is a nature reserve near the town of Abisko, Sweden. The site is located 200 km north of the Arctic Circle and 385 m asl. July, with an average temperature of 11°C, is the warmest month of the year and at this latitude daylight is continuous. The subarctic mire is in a zone of discontinuous permafrost and consists of a mosaic of elevated ombrotrophic and lower-lying minerotrophic parts, surrounded by mountain birch forest [*Svensson et al.*, 1999; *Johansson et al.*, 2006]. Tundra vegetation covers the upper slopes of the mountains in the region. Stordalen is accessible only by foot or helicopter and is located 1 km to the east of the E10 roadway. The E10 is a two- to four-lane road, the area's largest, which connects Narvik, Norway, and Kiruna, Sweden (both are ~90 km from Stordalen in opposite directions). One kilometer to the east of Stordalen is Lake Torneträsk, and 10 km to the west is the village of Abisko (permanent population ~150). Electric railroads in the Abisko area are regularly used, 10–12 times per day, for open freight shipping of iron ore from Kiruna to the port at

Narvik. The rail line and domestic heating are the largest local anthropogenic sources of gases and particles. To the east of the Abisko region lies northern Finland, Russia, and the Barents Sea; this includes the industrial area of the Kola Peninsula. The topography is relatively flat, with altitudes mostly below 500 m asl. To the north, west, and southwest, the region borders the 1000–2000 m asl. Scandinavian Mountains. Beyond the Scandinavian Mountains is the Norwegian Sea. The entire region is sparsely populated and much of the area is held in nature preserves. A regional map of the Abisko area, including vegetation zones, can be found in Figure 1 of *Svenningsson et al.* [2008]. In summary, the Stordalen site allows access to Arctic air masses with few local anthropogenic sources. Depending upon wind direction and meteorology particulate sources from both natural (e.g., oceanic and boreal forest) and anthropogenic (e.g., the port at Narvik and industries on the Barents Sea) sources are expected to perturb the background conditions.

[10] The Lagrangian trajectory model LAGRANTO [*Wernli and Davies*, 1997], which uses meteorological analyses from the European Center for Medium-Range Weather Forecasts (ECMWF), was used to determine the air mass history during the study period. Available on standardized time intervals (0000, 0600, 1200, and 1800 UTC) on 91 model levels, the data is superimposed on a fixed Gaussian grid ($0.25^\circ \times 0.25^\circ$). The position of the air parcels is determined from a three-dimensional wind field; standard trajectories were calculated 48 h back for every day for 1200 UTC and 0000 UTC arrival time at the field site (at 385 m asl). These back trajectories show three main stable air masses during the sampling period that originated from the south, northeast, and west, respectively. Short periods of "unsettled flow" occurred between these stable periods and are removed from this data set. Sampling times, air mass information, SMPS data, daily averaged trajectories and site-related meteorological information are shown in Figure 1.

2.3. Instrumentation

[11] During the month of July 2007, aerosol instrumentation was located within a $\sim$25 m^2 cabin at a field site located at Stordalen mire, approximately 10 km from the Abisko Scientific Research Station operated by the Royal Swedish Academy of Sciences. More details are given in section 2.4. Ambient aerosol particles entered the cabin through an isokinetic PM-10 inlet (URG, Model 2000–30DBQ). The output of the PM-10 inlet was then split into four lengths of 6-mm-diameter capillary tubing directed to a CPC (flow rate = 1 L/min, 10 nm to 3 μm diameter range, TSI Model 3772 for first two measurement weeks, thereafter a TSI Model 3010), an ATOFMS (flow rate = 0.1 L/min), a CCNC (flow rate = 0.5 L/min, Droplet Measurement Technologies), and a custom-built HTDMA based on the instrument described by *Weingartner et al.* [2002] with a CPC (TSI, Model 3010, flow rate = 1 L/min). An additional flow of 5 L/min was added to achieve the desired cut point of the inlet. Tube lengths were such that equal transit times occurred from the inlet to each instrument. When the HTDMA and ATOFMS were connected in series, or when instruments were periodically cleaned, calibrated, or changed, extra tubes were capped. A custom built SMPS (size range 10–550 nm diameter), which operates continuously at the Stordalen site, draws particles from a separate inlet system. A complete description of this system is given by *Svenningsson et al.* [2008]. In this manner, particle concentration was determined from the CPC, the size distribution from the SMPS, the hygroscopic properties from the HTDMA, the cloud nuclei concentration from the CCNC, and the chemical composition of single particles was determined by the ATOFMS. In total, $\sim$70,000 ambient single particle mass spectra were obtained in the size range between $\sim$200 and 2000 nm.

[12] The ATOFMS is a single particle mass spectrometer described in detail by *Gard et al.* [1997]. Briefly, particles are drawn into the instrument through an aerodynamic lens and are accelerated such that their velocity is a function of their aerodynamic diameter [*Liu et al.*, 1995a, 1995b]. After two differential pumping stages the particles scatter light as they travel through two diode-pumped neodymium-doped yttrium aluminum garnet (Nd:YAG) continuous sizing lasers (λ = 532 nm). These two Nd:YAG sizing lasers are situated at a known distance apart from each other. The scattering signals of the lasers are detected with two photomultipliers, allowing for a calculation of the particle flight velocity, and thus the vacuum aerodynamic diameter of the particle. Using polystyrene latex spheres of known size for calibration, it was observed that the detectable scattering of light by particles set a lower threshold of $\sim$200 nm diameter whereas efficient detection was not observed until >250 nm. The focus of the aerodynamic lens falls off above 600 nm diameter and no particles were observed above 2000 nm during this study. Particles next pass into a mass spectrometer region where the fourth harmonic of a pulsed Nd:YAG (λ = 266 nm) laser acts to desorb and ionize the aerosol. The firing of the desorption and ionization (DI) laser is dependent on the calculated particle flight velocity. Generated ions are then accelerated into one of two time-of-flight mass spectrometers according to their polarity. In this way positive and negative mass spectra are obtained in situ and in real time at the single particle level. Volatile, semivolatile and refractory components are resolved with this technique.

[13] The ATOFMS should be considered a qualitative instrument. The peak areas in the ATOFMS bipolar mass spectra result from ions generated by the DI laser beam. Ion generation can be impacted by the distribution of components through the aerosol, the ionization efficiency of the specific materials, as well as other properties of the particle matrix [*Gross et al.*, 2000; *Murphy*, 2007]. Thus, without laboratory determination of these "matrix effects" mass spectral peak areas cannot be directly related to the component quantities [*Cziczo et al.*, 2001; *Dessiaterik et al.*, 2003].

[14] The experimental timeline is illustrated in Figure 1. Periods when the ATOFMS was connected in series to the HTDMA (Figure 1a, purple squares) are discussed by *Herich et al.* [2009]. Comparisons of aerosol hygroscopicity and cloud condensation nuclei during parallel sampling of the HTDMA (Figure 1a, bright yellow squares) are the subject of Kammermann et al. (manuscript in preparation, 2009).

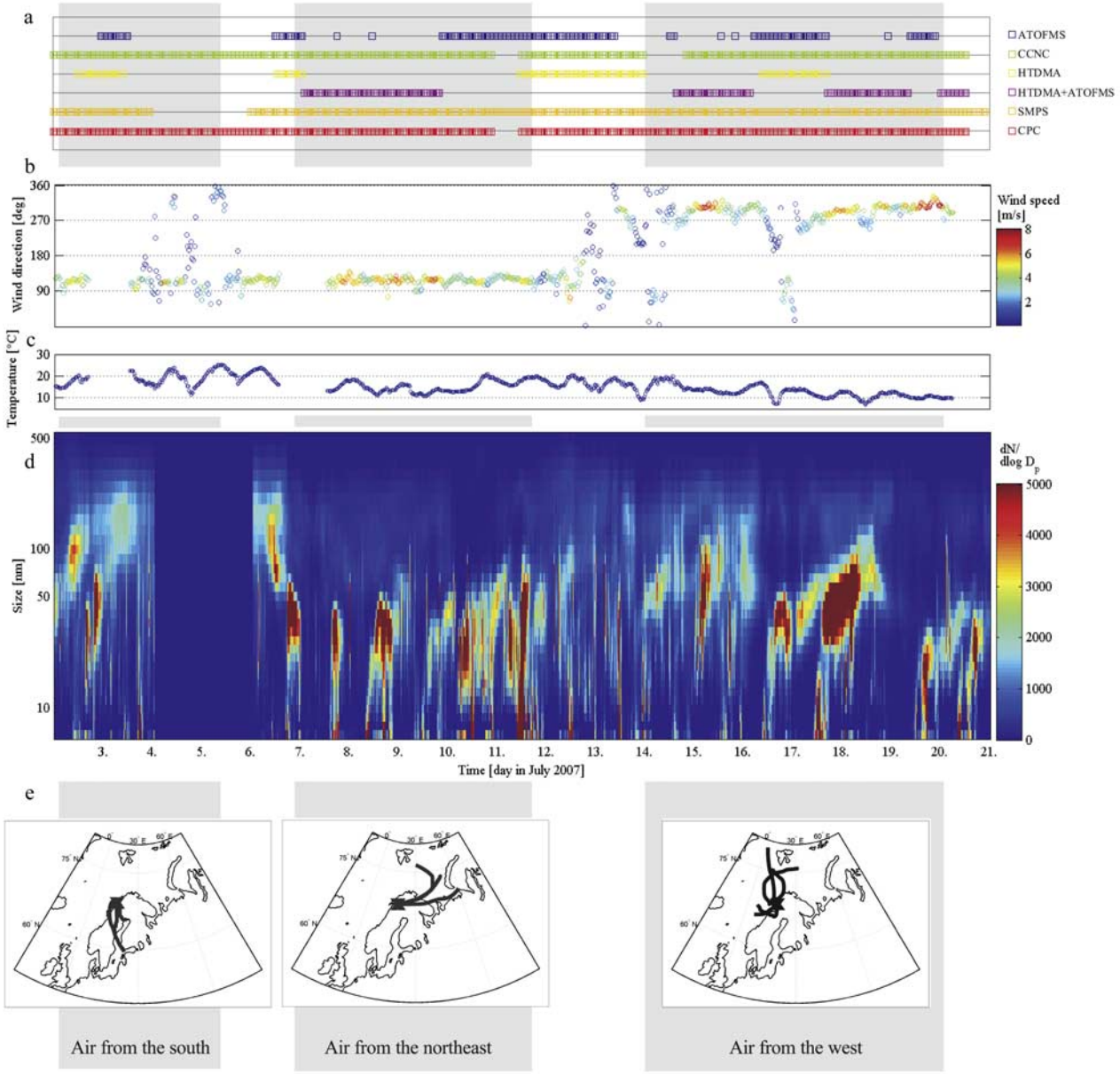

Figure 1. Ambient aerosol and meteorological data at the Stordalen field site during the month of July 2007. (a) Time periods within the month during which each instrument was operating. (b) Wind direction and speed, (c) virtual temperature, and (d) size-resolved particle concentration measured with an SMPS. It should be noted that this is a local wind direction and wind speed data that need not correlate with the back trajectory wind fields. (e) The three distinct air masses that were sampled, correlating with the shaded time periods in Figure 1a. Back trajectories, one per day within each air mass, are plotted on a Scandinavian projection.

2.4. Cluster Analysis

[15] ATOFMS analysis was performed by the data mining program ENvironmental CHemistry through InteLligent Atmospheric Data Analysis (ENCHILADA) developed at Carleton College and the University of Wisconsin-Madison (D. S. Gross et al., ENCHILADA: Environmental chemistry through intelligent atmospheric data analysis, submitted to *Environmental Modeling and Software*, 2009). ENCHILADA allows for the analysis of particle mass spectra and time series using data mining and visualization tools. Aerosol particle data is clustered through a K-means algorithm. The K-means clustering algorithm assigns each particle to a cluster whose center is nearest in Euclidean space. The center is an average of all the particles in the cluster, and is thus indicative of a grouping of similar particles. The algorithm assigns particles to a given cluster and then recomputes a new center; the algorithm is only finished when the error (defined as the distance between all particles and their assigned cluster centers) is minimized and all particle data points have been assigned to a cluster. At common atmospheric aerosol number densities

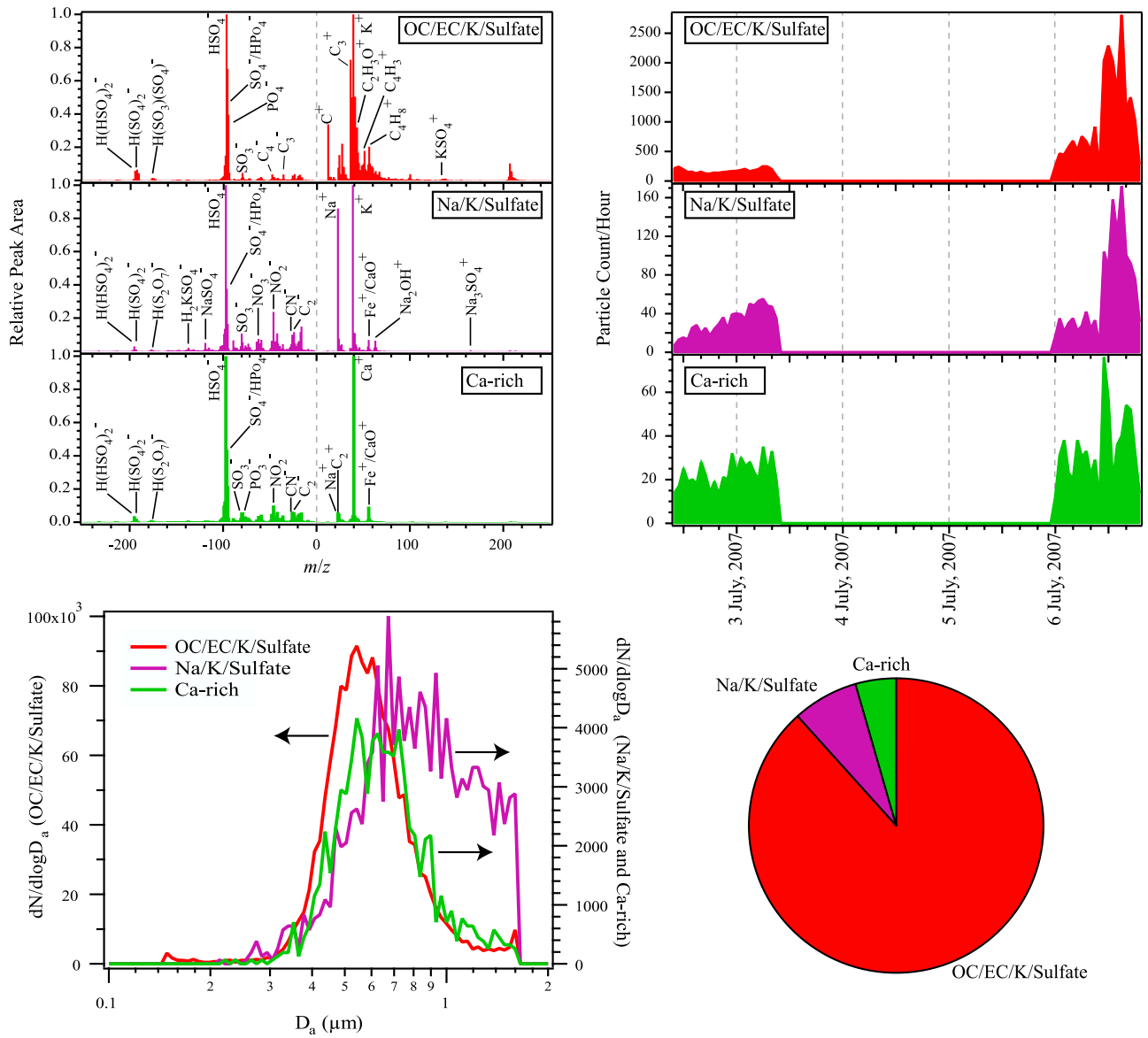

Figure 2. Chemical composition and size information for the ambient aerosol within an air mass originating to the south of the Stordalen field site. (top left) The average bipolar ion spectra for three cluster centers. (top right) The particle acquisition rate for these three clusters as a function of time. Note that the ATOFMS was not run for ~48 h from 3 to 5 July as a connection to the HTDMA was tested. Note also that data on 6 July are from a transition period to an air mass from the northeast. (bottom left) The occurrence of particle type according to aerodynamic size (obtained by the ATOFMS), with the OC/EC/K/Sulfate cluster size distribution shown on the left-hand *y* axis and the other clusters all shown on the right-hand *y* axis, as indicated by the arrows. (bottom right) A number-based pie chart of the aerosol clusters during this air mass. The full pie stands for the total number of spectra acquired during this air mass.

a single particle instrument can produce tens of thousands of mass spectra per day; cluster analysis allows handling of the composition of large data sets by grouping similar particle types. By setting the value for K, or the number of clusters to group particles into, the user can control how coarse or fine the subdivisions between clusters are. In this study, we used the smallest number of clusters which adequately defined the data set, based on small changes upon increasing K. For the purpose of the data set obtained in this field study, mass spectra were subdivided according to air mass origin before clustering, as specified in section 3.

[16] During this field study, three, three, and five clusters were found to most readily delineate the spectra acquired in the south, northeast, and west air masses, respectively. In all three air masses, the most populous cluster contained organic carbon (OC), elemental carbon (EC), potassium (K) and sulfates. These components were found internally mixed in various ratios (i.e., any could represent the largest or smallest signal). The other clusters were differentiated by components such as mineral dust or sea salt. It is noteworthy that the delineation was thus most clearly shown by a refractory component of the particle (e.g., EC, mineral dust,

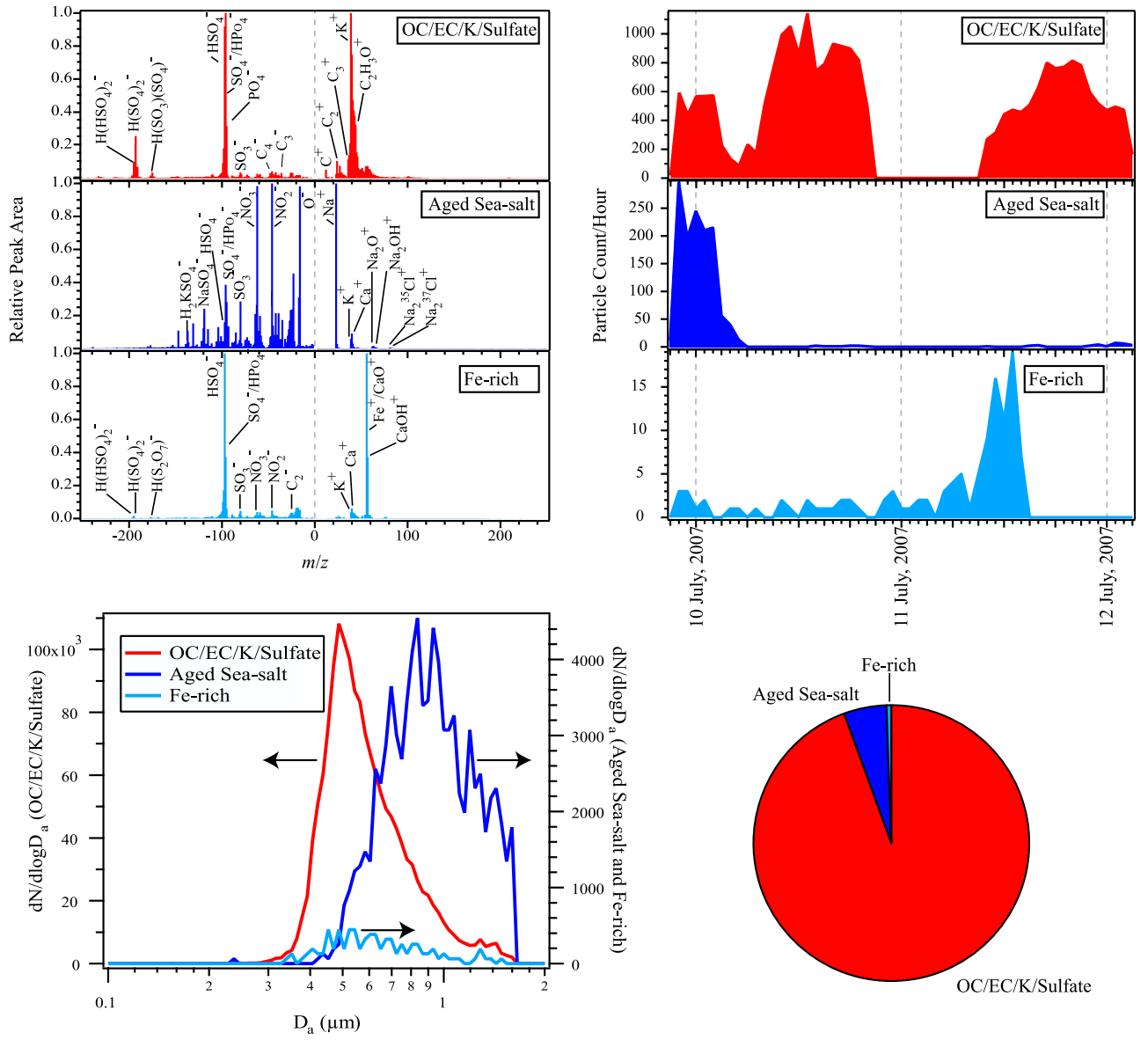

Figure 3. Chemical composition and size information for the ambient aerosol within an air mass originating to the northeast of the Stordalen field site. Panels are as defined in Figure 2 although note that the three cluster centers are different. Note also that the ATOFMS was connected to the HTDMA for the early portion of this air mass.

and sea salt). Such a delineation would not have been apparent in previous Arctic studies of aerosol with an AMS instrument which cannot resolve refractory compounds [*Allan et al.*, 2006; *Drewnick et al.*, 2007].

[17] To test the need for more clusters, ENCHILADA was also run with a fixed number of 30 cluster centers for each of the three air masses. In all three air masses a single large cluster was produced which encompassed 67, 71, and 76% of all particles for the South, Northeast, and West air masses, respectively; this cluster was OC/EC/K/Sulfates. Furthermore, less than 10 total clusters represented greater than 99% of all particles in all three air masses. That is to say that even though 30 centroids were used, only 10 were required to cluster essentially all of the particles. Furthermore, by forcing a requirement for more clusters groups that would normally cluster together were split. For example, clusters with OC, EC, potassium, and sulfate were split such that the magnitude of one component or another (e.g., a large sulfate or organic signal) differentiated the cluster. Since these four species existed as a continuum in this data set this arbitrary subclustering did not accurately reflect the distribution of mass spectra. Thus, the clusters discussed in the previous paragraphs and indicated in Figures 2, 3, and 4 are considered the best overall representation of this data set.

3. Results

3.1. Air Mass South

[18] Initial ambient sampling commenced on 2 July 2007. The air mass at the outset of the study, from 2 to 6 July, exhibited a back trajectory that passed along the Scandinavian Peninsula from south to north (Figure 1). Local winds

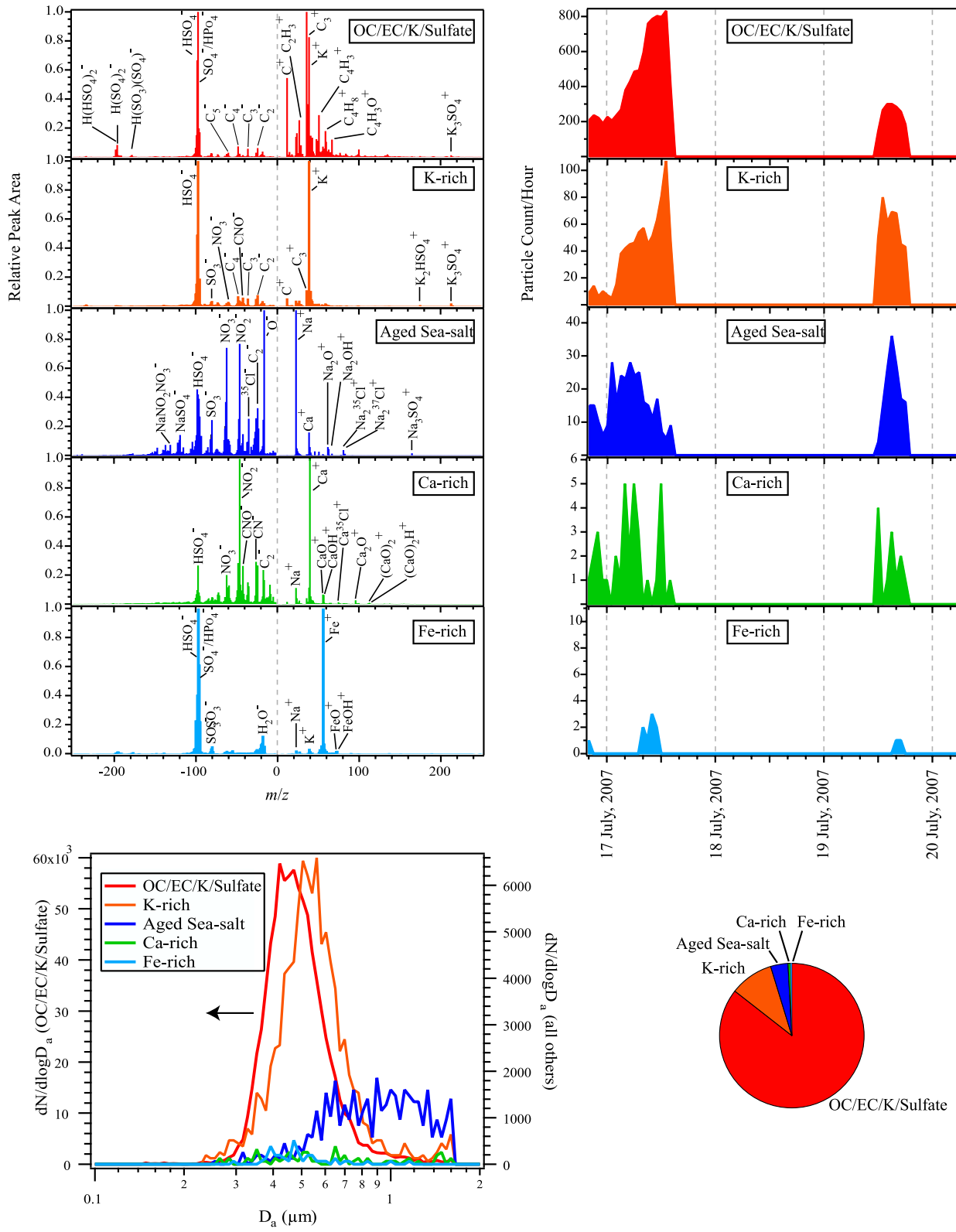

Figure 4. Chemical composition and size information for the ambient aerosol within an air mass originating to the west of the Stordalen field site. Panels are as defined in Figure 2 although note that there are five different cluster centers for this air mass. Note also that the ATOFMS was connected to the HTDMA during approximately the first and third quarters of this air mass.

Table 1. Characteristic Ions for the Clusters Found in the Three Air Masses Measured, Including the Percentage of Particles Assigned to Each Cluster

Cluster Name	Characteristic Ions	Percentage in Air Mass		
		South	Northeast	West
OC/EC/K/sulfate	C^+, C_2^+, $C_2H_3^+$, C_3^+, K^+, C_4^+, KNO_3^+, C_2^-, C_3^-, C_4^-, SO_3^-, SO_4^-, HSO_4^-, $H(HSO_4)_2^-$	88	91	86
Na/K/sulfate	Na^+, K^+, Na_2O^+, Na_2OH^+, O^-, C_2^-, NO_2^-, NO_3^-, SO_3^-, HSO_4^-, $NaSO_4^-$	7		
Ca-rich	Na^+, Ca^+, CaO^+, $CaOH^+$, Ca_2O^+, $CaNO_3^+$, O^-, OH^-, NO_2^-, NO_3^-, SO_3^-, HSO_4^-, $HS_2O_7^-$	5		<1
Aged sea salt	Na^+, K^+, Na_2^+, Na_2O^+, Na_2OH^+, O^-, Cl^-, NO_2^-, NO_3^-, SO_3^-, $NaNO_3^-$, $NaCl_2^-$, SO_4^-, HSO_4^-		5	4
Fe-rich	Na^+, K^+, V^+, Fe^+, VO^+, $FeOH^+$, $FeOH^+$, SO_3^-, SO_4^-, HSO_4^-		4	<1
K-rich	C^+, Na^+, $C_2H_3^+$, C_3^+, K^+, $K_2HSO_4^+$, C_2^-, C_3^-, CNO^-, C_4^-, SO_4^-, HSO_4^-, $K(HSO_4)_2^-$			9

were also predominantly from the south and we therefore term this "air mass south" and note that it was followed by ~24 h of unsettled flow direction. This period was characterized by the highest particle numbers in the size range above 250 nm diameter, with total concentrations of 3000 per cm^3 or greater. Note that the majority of the aerosol number at all times remained in the size range below 250 nm. The numbers above this size were largely unaffected by nucleation events and the number concentrations in this range were always below 500 per cm^3. In this air mass the SMPS data appears to indicate a new particle formation event between 2 and 3 July. The ATOFMS sampled for a period at the beginning and end of this air mass with no sampling in the middle while connections to the HTDMA were tested. A total of 27,651 ambient aerosol mass spectra from this air mass were obtained.

[19] Using ENCHILADA, three cluster centers were found to best define the air mass. The results for these three clusters are shown in Figure 2. The largest cluster, on a number basis, exhibited spectral peaks of OC, EC, K and sulfate in variable ratios indicating an internal mixture of these components. This is most probably primary aerosol particles from combustion (EC) and biomass burning (K) which contained or took up from the gas phase organic carbon and sulfate. Specific characteristic peaks are listed in Table 1. The location of population centers in southern Scandinavia with large tracts of boreal forest between there and Stordalen is consistent with this viewpoint. The OC/EC/K/Sulfate aerosol had little variability within this air mass until an increase with the onset of unsettled flow on 6 July. The mode size of this aerosol as measured by the ATOFMS was relatively small compared to the other clusters, centered at ~500 nm aerodynamic diameter. Particles of this type were found from the lowest size detected with the ATOFMS (~200 nm) to the highest (~2000 nm). In total, OC/EC/K/Sulfate particles made up 88% of the total analyzed in air mass south.

[20] The second most numerous cluster is particles with dominant positive sodium and potassium peaks (see Table 1 for mass peak details). This cluster had the largest mode of the three, ~750 nm diameter, but extending to the upper detection limit of the ATOFMS. Cluster 2 comprised 7% of the total particles in air mass south. The relative ratios and internally mixed sodium, potassium, and sulfate compounds in these particles do not correlate with common clusters found in other locations. An electron microscope study in Finland by *Niemi et al.* [2006] noted the presence of large (PM1–3.3) "sponge-like" particles which contained Na, S, K, and O which they attributed to burning in the wood pulp/paper industry. The southern origin during this period does coincide with industries of this type, suggesting this as a possible source for these particles.

[21] The least populous cluster is termed calcium-rich owing to the dominance of this positive ion in the spectra (Table 1). Calcium particles likely originated from mineral dust which took up gas phase sulfate and nitrate compounds [*Laskin et al.*, 2005]. There was a slight increase in the abundance of this particle type over the period of this air mass with a peak in the unsettled flow at the end. These particles, with an ATOFMS-measured mode at ~650 nm, were larger than the OC/EC/K/Sulfate but smaller than the Na/K/Sulfate cluster presumably originating from the wood pulp/paper industry. The calcium cluster made up 5% of the total in air mass south.

3.2. Air Mass Northeast

[22] After ~24 h of unsettled flow from 6 to 7 July the back trajectories indicate a steady flow from the northeast until 12 July. We therefore define this as "air mass northeast" although we note that local winds were variable with a southerly component. This period was characterized by lower particle densities than during "air mass south," ~500 per cm^3, and a smaller mode size, ~50 nm. Particle concentrations were in general on the order of 3000 per cm^3 while concentrations above 250 nm were below 300 per cm^3. New particle formation events occurred sporadically during this period. The ATOFMS was connected to the HTDMA for joint sampling during most of the first 3 days within this air mass. Dedicated ambient sampling from 10 to 12 July produced 26,840 mass spectra from air mass northeast.

[23] Three main cluster types were identified for this air mass. The results for these three clusters are shown in Figure 3. On a number basis the largest cluster was OC/EC/K/Sulfate, similar in nature to the predominant cluster in air mass south. Specific peaks are listed in Table 1. The OC/EC/K/Sulfate aerosol exhibited a sharp mode at ~500 nm diameter although particles were detected to the lower and upper thresholds of the ATOFMS. OC/EC/K/Sulfate particles were detected at the start and end of the ambient sampling in this air mass with a noticeable void on 11 July due to local precipitation. With 8 mm rainfall over 8 h, this was the largest precipitation event of the experimental period. The OC/EC/K/Sulfate cluster comprised 91% of particles in air mass northeast.

[24] The second most populous cluster in air mass northeast comprises sea salt (Table 1). The observed peaks are indicative of aged sea salt. Sea salt aerosol can participate in

a heterogeneous reaction with gaseous HNO_3 which leads to a replacement of chloride by nitrates, thus explaining the presence of strong NO_2^- and NO_3^- peaks, with smaller magnitude $^{35}Cl^-$ and $^{37}Cl^-$ [*Gard et al.*, 1997]. The aged sea salt was almost exclusively evident in the first day of ambient sampling from this air mass although it was also apparent earlier in the combined HTDMA-ATOFMS study. The mode size of the sea salt particles was the largest of those observed, peaking at ~1000 nm and extending to the upper threshold of the ATOFMS. Aged sea salt comprised 5% of the total particles sampled in air mass northeast.

[25] Instead of particles with a dominant positive calcium ion a class of particles with a large iron peak was observed in air mass northeast. This cluster is therefore termed iron-rich. While CaO^+ and Fe^+ coexist in a mass spectrum, the relative lack of Ca^+ indicates that Fe^+ was dominant. The existence of positive peaks at mass 54 and 57, stable isotopes of iron, support this identification. See Table 1 for specific peak details. It is noteworthy that the large Kiruna iron ore mine lies to the east and the ore rail line passes near the Stordalen field site, providing a reasonable source for these particles. The nitrate, sulfate, and organic ions in the spectra may indicate uptake from the gas phase during their transport to the Abisko region. The particles were observed through the first two days of ambient sampling in air mass northeast with a peak observed on 11 July. In total 4% of the particles in the air mass were clustered into this class.

3.3. Air Mass West

[26] An unsettled flow was identified for the period of 12–14 July. This was followed by a flow from 16 to 20 July with back trajectories to the west, northwest, and north. Local winds were predominantly from the west and we hereafter term this period, for simplicity, "air mass west." The particle number density in this air mass was variable, ranging from 100 to 7000 per cm^3, as was the aerosol size, with modes from <50 nm to >100 nm in mobility diameter. Particle concentrations in the size range above 250 nm were below 500 per cm^3.The combined HTDMA-ATOFMS setup was employed during approximately the first and third quarters of air mass west with ambient sampling otherwise. Ambient data was also taken for a short period on 19 July which was otherwise committed to the combined setup. In total, 15,315 mass spectra of ambient particles were obtained from air mass west.

[27] For air mass west, five clusters were used to fit the mass spectra. The results for these five clusters are shown in Figure 4. The numerically largest of these was similar to the OC/EC/K/Sulfate cluster found in air mass south and northeast. Specific peaks are listed in Table 1. The OC/EC/K/Sulfate cluster was the most numerous throughout the sampling period and, with a ~500 nm ATOFMS mode, the smallest. The OC/EC/K/Sulfate cluster comprised 86% of the aerosol in air mass west.

[28] The second most abundant cluster is termed potassium-rich owing to the dominance of this positive ion. Mass peaks are listed in Table 1. This class of potassium-rich spectra has been previously correlated with relatively fresh biomass burning emissions [*Hudson et al.*, 2004]. The location of the village of Abisko, as well as the larger port of Narvik, to the west of Stordalen, supports a local domestic heating source contributing to this aerosol during predominantly westerly flow. Potassium-rich particles were the second most abundant throughout this period and also the second smallest, with an ATOFMS mode size between 500 and 600 nm (i.e., just larger than the OC/EC/K/Sulfate cluster). This cluster comprised 9% of the total particles of air mass west.

[29] The third cluster was similar to the second most abundant cluster in air mass northeast, aged sea salt (see Table 1 for specific mass peaks). The presence of relatively strong nitrate and weak chlorine and sodium chloride peaks in the negative ion spectra define this as aged, not fresh, sea salt. The mode size, ~1000 nm with particles extending to the upper ATOFMS size threshold, is also consistent with aged sea salt. This cluster made up 4% of the total particles in air mass west.

[30] The fourth and fifth clusters had approximately the same abundance, ~0.5% of the total aerosol in air mass west. The fourth cluster exhibited a strong Ca^+ peak (Table 1). Calcium-rich particles were sampled throughout the period although they appeared in sporadic peaks, the largest at the end of the sampling time. The Ca-rich particles were large, with a broad ATOFMS mode from ~300 to 2000 nm. The fifth was an iron-rich cluster. The positive ion spectra exhibit a dominant peak at m/z = 56, corresponding to iron. The lack of a large Ca^+ peak as well as iron isotopes at positive mass 54 and 57 support this identification (Table 1). Iron-rich particles also were observed sporadically throughout air mass west with a large peak toward the end of the sampling period. This cluster also had a broad ATOFMS size mode from ~300 to 2000 nm.

4. Air Mass Comparison and Atmospheric Implications

[31] The technique of SPMS has been employed for field studies of atmospheric aerosols since the mid-1990s [*Murphy and Thomson*, 1997a, 1997b]. An airborne instrument has acquired data from ground level to ~19 km altitude from a variety of platforms and at a number of locations [*Murphy et al.*, 1998, 2006]. The commercialization of this technology within the last decade has allowed for an increase in data sets with essentially the same instrument technology, thus making intercomparisons more accurate [*Gard et al.*, 1997; *Suess and Prather*, 1999; *Nash et al.*, 2006]. Regardless, the difficulty of access and a dearth of organized field missions at high northern and southern latitudes have resulted in a complete lack of SPMS aerosol data in the Arctic and Antarctic. This is despite the fact that aerosol size, composition, and mixing state play important roles in atmospheric chemistry, visibility, and direct and indirect climatic effects.

[32] The foremost result of this study is that high-latitude aerosol is not altogether different from free tropospheric aerosol found at midlatitudes. Aircraft [*Murphy et al.*, 2006] and mountaintop studies [*DeMott et al.*, 2003] using SPMS have also found that the majority of atmospheric aerosol in the 200- to 2000-nm aerodynamic diameter size range are internal mixtures of sulfates and organics with some 30–80% containing a nonvolatile core that cannot be attributed to condensation of gas phase material. The data presented here suggest that long-range transport, and not a local

source, was responsible for most of the analyzed particles. Nonvolatile cores included material from biomass burning, elemental carbon likely from combustion processes, and mineral dust. The agreement among air masses of different directions (south, northeast, and west) indicates that this type of aerosol likely exists throughout the Arctic during the summer season.

[33] Local sources are nonetheless important in the Arctic. Despite the general view that the region in sparsely inhabited some of these sources are anthropogenic. Spectra associated with the wood pulp and paper industry [*Niemi et al.*, 2006] were indicated during southerly flow. Aerosols with a mineral signature made up from 1 to 5% of the total by number of the analyzed aerosol. The composition of the aerosol changed with the air mass; Ca-rich aerosol predominated with southern flow whereas Fe-rich particles were observed in northeastern flow. Both particle types showed signs of gas-phase uptake of nitrates [*Laskin et al.*, 2005] as has been observed in other atmospheric SPMS studies [*Murphy et al.*, 2006]. It is noteworthy that the Kiruna iron ore mine is located to the east of the Stordalen, the electrically powered ore rail line passes within ~2 km distance from the sampling site, and the industrial and port city of Murmansk lies to the northeast. Any of these may be the source of iron-rich particles which were observed in the air mass northeast and west, but not in air mass south. The lowest abundance of particles with a mineral signature occurred in air mass west although both Ca- and Fe-rich particles were observed at the sub-1% level. This may be more closely related to the background level in the Arctic and it is similar to that found in free tropospheric studies on a mountaintop in the midlatitudes [*DeMott et al.*, 2003]. The composition of mineral dust is of interest since it dictates some heterogeneous chemical reactions [*Laskin et al.*, 2005] and ice nucleation [*Gallavardin et al.*, 2008].

[34] Sea salt was observed at a higher abundance in the data from Stordalen than in free-tropospheric aerosol at midlatitudes. This is not unexpected since the Scandinavian Peninsula is largely surrounded by the open ocean during the summer season. One surprising result was that the abundance of sea salt, 4–7%, was observed to be low for the air mass most directly originating from open ocean, that from the west. The relative lack of sea salt is most likely due to wet deposition during precipitation as air mass west passed over the Norwegian coastal mountain range. This concept is expanded in the companion paper on hygroscopicity by *Herich et al.* [2009]. Whereas OC/EC/K/Sulfate and mineral dust aerosol likely exists throughout the Arctic, sea salt may not be homogenously distributed. The proximity of the site to open ocean as well as topographic features and meteorology likely determine the abundance of sea salt aerosol.

[35] Essentially all analyzed aerosol can be considered well-aged and internally mixed. Most contained some organic material. Some of this material may have been present during formation for biomass, EC, and sea salt particles. With essentially continuous daylight the summer season is the annual peak for gas-phase emissions from plants in the Arctic. Furthermore, the relatively lower temperature in the Arctic (~12°C average temperature at Stordalen during July 2007) may lead to more partitioning of semivolatile compounds to the condensed phase than would be found at lower latitudes. This production of gas-phase organic compounds is highly dependent on the season and does not occur during the winter. Likewise, ice and snow cover during the winter likely reduces sea salt and aeolian-produced mineral dust. We suggest the need for more studies in the Arctic to elucidate the distribution of aerosol types as well as the annual cycle, which is likely far more pronounced than in the midlatitudes.

[36] **Acknowledgments.** This work was supported by ETH internal research funding, the PNNL Aerosol Initiative, the Royal Swedish Academy of Sciences, Carleton College, and a European Commission/Marie Curie Excellence grant. We thank the staff at the Abisko Scientific Research Station for logistical assistance. We appreciate Markus Gälli for ATOFMS technical support and Andreas Mühlbauer and Peter Spichtinger for providing trajectory data.

References

Albrecht, B. (1989), Aerosols, cloud microphysics, and fractional cloudiness, *Science*, *245*, 1227–1230, doi:10.1126/science.245.4923.1227.

Allan, J. D., et al. (2006), Size and composition measurements of background aerosol and new particle growth in a Finnish forest during QUEST 2 using an aerodyne aerosol mass spectrometer, *Atmos. Chem. Phys.*, *6*, 315–327.

Baltensperger, U., et al. (2002), Urban and rural aerosol characterization of summer smog events during the PIPAPO field campaign in Milan, Italy, *J. Geophys. Res.*, *107*(D22), 8193, doi:10.1029/2001JD001292.

Behrenfeldt, U., R. Krejci, J. Ström, and A. Stohl (2008), Chemical properties of Arctic aerosol particles collected at the Zeppelin station during the aerosol transition period in May and June of 2004, *Tellus, Ser. B*, *60*, 405–415.

Bond, T. C., and R. W. Bergstrom (2006), Light absorption by carbonaceous particles: An investigative review, *Aerosol Sci. Technol.*, *40*, 27–67, doi:10.1080/02786820500421521.

Chýlek, P., and J. A. Coakley Jr. (1974), Aerosols and climate, *Science*, *183*, 75–77, doi:10.1126/science.183.4120.75.

Coakley, J. A., Jr., R. E. Cess, and F. B. Yurevich (1983), The effect of tropospheric aerosols on the Earth's radiation budget: A parameterization for climate models, *J. Atmos. Sci.*, *40*, 116–138, doi:10.1175/1520-0469(1983)040<0116:TEOTAO>2.0.CO;2.

Cziczo, D. J., D. S. Thomson, and D. M. Murphy (2001), Ablation, flux, and atmospheric implications of meteors inferred from stratospheric aerosol, *Science*, *291*, 1772–1775, doi:10.1126/science.1057737.

DeMott, P. J., D. J. Cziczo, A. Prenni, D. M. Murphy, S. Kreidenweis, D. S. Thomson, and R. Borys (2003), Compositions and concentrations of atmospheric ice nuclei, *Proc. Natl. Acad. Sci. U. S. A.*, *100*, 14,655–14,665, doi:10.1073/pnas.2532677100.

Dessiaterik, Y., T. Nguyen, T. Baer, and R. E. Miller (2003), IR vaporization mass spectrometry of aerosol particles with ionic solutions: The problem of ion-ion recombination, *J. Phys. Chem. A*, *107*, 11,245–11,252, doi:10.1021/jp036171i.

Dibb, J. E., R. W. Talbot, S. I. Whitlow, M. C. Shipham, J. Winterle, J. McConnell, and R. Bales (1996), Biomass burning signatures in the atmosphere and snow at Summit, Greenland: An event on 5 August 1 994, *Atmos. Environ.*, *30*, 553–561, doi:10.1016/1352-2310(95)00328-2.

Drewnick, F., J. Schneider, S. S. Hings, N. Hock, K. Noone, A. Targino, S. Weimar, and S. Borrmann (2007), Measurement of ambient interstitial and residual aerosol particles on a mountaintop site in central Sweden using an aerosol mass spectrometer and a CVI, *J. Atmos. Chem.*, *56*, 1–20, doi:10.1007/s10874-006-9036-8.

Dusek, U., et al. (2006), Size matters more than chemistry for cloud-nucleating ability of aerosol particles, *Science*, *312*, 1375–1378, doi:10.1126/science.1125261.

Gallavardin, S., et al. (2008), Single particle laser mass spectrometry applied to differential ice nucleation experiments at the AIDA chamber, *Aerosol Sci. Technol.*, *42*, 773–783, doi:10.1080/02786820802339538.

Gard, E., J. E. Mayer, B. D. Morrical, R. Dienes, D. P. Fergenson, and K. A. Prather (1997), Real-time analysis of individual atmospheric aerosol particles: Design and performance of a portable ATOFMS, *Anal. Chem.*, *69*, 4083–4091, doi:10.1021/ac970540n.

Gross, D. S., M. E. Gälli, P. J. Silva, and K. A. Prather (2000), Relative sensitivity factors for alkali metal and ammonium cations in single-particle aerosol time-of-flight mass spectra, *Anal. Chem.*, *72*, 416–422, doi:10.1021/ac990434g.

Hegg, D. A., D. S. Covert, K. K. Crahan, H. H. Jonsson, and Y. Liu (2006), Measurements of aerosol size-resolved hygroscopicity at sub and supermicron sizes, *Geophys. Res. Lett.*, *33*, L21808, doi:10.1029/2006GL026747.

Heintzenberg, J. (1980), Particle size distribution and optical properties of Arctic haze, *Tellus*, *32*, 251–260.

Herich, H., L. Kammermann, B. Friedman, D. S. Gross, E. Weingartner, U. Lohmann, P. Spichtinger, M. Gysel, U. Baltensperger, and D. J. Cziczo (2009), Subarctic atmospheric aerosol composition: 2. Hygroscopic growth properties, *J. Geophys. Res.*, *114*, D13204, doi:10.1029/2008JD011574.

Hu, J. H., and J. P. D. Abbatt (1997), Reaction probabilities for N_2O_5 hydrolysis on sulfuric acid and ammonium sulfate aerosols at room temperature, *J. Phys. Chem.*, *101*, 871–878, doi:10.1021/jp9627436.

Hudson, P. K., D. M. Murphy, D. J. Cziczo, D. S. Thomson, J. A. de Gouw, C. Warneke, J. Holloway, H.-J. Jost, and G. Hübler (2004), Biomass burning particle measurements: Characteristic composition and chemical processing, *J. Geophys. Res.*, *109*, D23S27, doi:10.1029/2003JD004398.

Intergovernmental Panel on Climate Change (IPCC) (2007), Climate Change 2007: The Physical Science Basis, in *Contribution of Working Group I to the Fourth Assessment Report of the Intergovernmental Panel on Climate Change*, Cambridge Univ. Press, Cambridge, U. K.

Johansson, T., N. Malmer, P. M. Crill, T. Friborg, J. H. Akerman, M. Mastepanov, and T. R. Christensen (2006), Decadal vegetation changes in a northern peatland, greenhouse gas fluxes and net radiative forcing, *Global Change Biol.*, *12*, 2352–2369, doi:10.1111/j.1365-2486.2006.01267.x.

Komppula, M., H. Lihavainen, V.-M. Kerminen, M. Kulmala, and Y. Viisanen (2005), Measurements of cloud droplet activation of aerosol particles at a clean subarctic background site, *J. Geophys. Res.*, *110*, D06204, doi:10.1029/2004JD005200.

Kulmala, M., et al. (2001), Overview of the international project on biogenic aerosol formation in the boreal forest (BIOFOR), *Tellus, Ser. B*, *53*, 324–343, doi:10.1034/j.1600-0889.2001.d01-24.x.

Kulmala, M., H. Vehkamaki, T. Petaja, M. Dal Maso, A. Lauri, V.-M. Kerminen, W. Birmili, and P. H. McMurry (2004), Formation and growth rates of ultrafine atmospheric particles: A review of observations, *J. Aerosol Sci.*, *35*, 143–176, doi:10.1016/j.jaerosci.2003.10.003.

Laskin, A., T. W. Wietsma, B. J. Krueger, and V. H. Grassian (2005), Heterogeneous chemistry of individual mineral dust particles with nitric acid: A combined CCSEM/EDX, ESEM, and ICP-MS study, *J. Geophys. Res.*, *110*, D10208, doi:10.1029/2004JD005206.

Lihavainen, H., V.-M. Kerminen, M. Komppula, J. Hatakka, V. Aaltonen, M. Kulmala, and Y. Viisanen (2003), Production of "potential" cloud condensation nuclei associated with atmospheric new-particle formation in northern Finland, *J. Geophys. Res.*, *108*(D24), 4782, doi:10.1029/2003JD003887.

Liu, P., P. J. Ziemann, D. B. Kittelson, and P. H. McMurry (1995a), Generating particle beams of controlled dimensions and divergence: I. Theory of particle motion in aerodynamic lenses and nozzle expansions, *Aerosol Sci. Technol.*, *22*, 293–313, doi:10.1080/02786829408959748.

Liu, P., P. J. Ziemann, D. B. Kittelson, and P. H. McMurry (1995b), Generating particle beams of controlled dimensions and divergence: II. Experimental evaluation of particle motion in aerodynamic lenses and nozzle expansions, *Aerosol Sci. Technol.*, *22*, 314–324, doi:10.1080/02786829408959749.

Lohmann, U., and J. Feichter (2005), Global indirect aerosol effects: A review, *Atmos. Chem. Phys.*, *5*, 715–737.

McCormick, R. A., and J. H. Ludwig (1967), Climate modification by atmospheric aerosols, *Science*, *156*, 1358–1359, doi:10.1126/science.156.3780.1358.

Mitchell, J. M. (1957), Visual range in the polar regions with particular reference to the Alaskan Arctic, *J. Atmos. Terr. Phys.*, *1957*, spec. suppl., 195–211.

Murphy, D. M. (2007), The design of single particle laser mass spectrometers, *Mass. Spectrom. Rev.*, *26*, 150–165.

Murphy, D. M., and D. S. Thomson (1997a), Chemical composition of single aerosol particles at Idaho Hill: Negative ion measurements, *J. Geophys. Res.*, *102*(D5), 6353–6368, doi:10.1029/96JD00859.

Murphy, D. M., and D. S. Thomson (1997b), Chemical composition of single aerosol particles at Idaho Hill: Positive ion measurements, *J. Geophys. Res.*, *102*(D5), 6341–6352, doi:10.1029/96JD00858.

Murphy, D. M., D. S. Thomson, and M. J. Mahoney (1998), In situ measurements of organics, meteoritic material, mercury, and other elements in aerosols at 5 to 19 kilometers, *Science*, *282*, 1664–1669, doi:10.1126/science.282.5394.1664.

Murphy, D. M., D. J. Cziczo, K. D. Froyd, P. K. Hudson, B. M. Matthew, A. M. Middlebrook, R. E. Peltier, A. Sullivan, D. S. Thomson, and R. J. Weber (2006), Single-particle mass spectrometry of tropospheric aerosol particles, *J. Geophys. Res.*, *111*, D23S32, doi:10.1029/2006JD007340.

Nash, D. G., T. Baer, and M. V. Johnston (2006), Aerosol mass spectrometry: An introductory review, *Int. J. Mass Spectrom.*, *258*, 2–12, doi:10.1016/j.ijms.2006.09.017.

Niemi, J. V., S. Saarikoski, H. Tervahattu, T. Mäkelä, R. Hillamo, H. Vehkamäki, L. Sogacheva, and M. Kulmala (2006), Changes in background aerosol composition in Finland during polluted and clean periods studied by TEM/EDX individual particle analysis, *Atmos. Chem. Phys.*, *6*, 5049–5066.

Penner, J. E., C. C. Chuang, and K. Grant (1998), Climate forcing by carbonaceous and sulfate aerosols, *Clim. Dyn.*, *14*, 839–851, doi:10.1007/s003820050259.

Quinn, P. K., et al. (2008), Short-lived pollutants in the Arctic: Their climate impact and possible mitigation strategies, *Atmos. Chem. Phys.*, *8*, 1723–1735.

Randles, C. A., L. M. Russell, and V. Ramaswamy (2004), Hygroscopic and optical properties of organic sea salt aerosol and consequences for climate forcing, *Geophys. Res. Lett.*, *31*, L16108, doi:10.1029/2004GL020628.

Suess, D. T., and K. A. Prather (1999), Mass spectrometry of aerosols, *Chem. Rev.*, *99*, 3007–3035, doi:10.1021/cr980138o.

Sullivan, R. C., and K. A. Prather (2005), Recent advances in our understanding of atmospheric chemistry and climate made possible by on-line aerosol analysis instrumentation, *Anal. Chem.*, *77*, 3861–3885, doi:10.1021/ac050716i.

Svenningsson, B., et al. (2008), Aerosol particle formation events and analysis of high growth rates observed above a subarctic wetland-forest mosaic, *Tellus, Ser. B*, *60*, 353–364.

Svensson, B. H., T. R. Christensen, E. Johansson, and M. Öquist (1999), Interdecadal changes in CO_2 and CH_4 fluxes of a subarctic mire: Stordalen revisited after 20 years, *Oikos*, *85*(1), 22–30, doi:10.2307/3546788.

Twomey, S. (1977), The influence of pollution on the shortwave albedo of clouds, *J. Atmos. Sci.*, *34*, 1149–1152, doi:10.1175/1520-0469(1977)034<1149:TIOPOT>2.0.CO;2.

Weingartner, E., et al. (2002), Hygroscopicity of aerosol particles at low temperatures. 1. New low-temperature H-TDMA instrument: Setup and first applications, *Environ. Sci. Technol.*, *36*, 55–62, doi:10.1021/es010054o.

Wernli, H., and H. C. Davies (1997), A Lagrangian-based analysis of extratropical cyclones. I: The method and some applications, *Q. J. R. Meteorol. Soc.*, *123*, 467–489, doi:10.1002/qj.49712353811.

A. Arneth and T. Holst, Department of Physical Geography and Ecosystems Analysis, Lund University, SE-22362 Lund, Sweden.

D. J. Cziczo, Atmospheric Science and Global Change, Pacific Northwest National Laboratory, 3200 Q Avenue, Richland, WA 99352, USA. (daniel.cziczo@pnl.gov)

B. Friedman, Department of Atmospheric Sciences, University of Washington, Seattle, WA 98195, USA.

D. S. Gross, Department of Chemistry, Carleton College, 1 North College Street, Northfield, MN 55057, USA.

H. Herich, Institute for Atmospheric and Climate Science, ETH Zurich, CH-8092 Zurich, Switzerland.

L. Kammermann, Laboratory of Atmospheric Chemistry, Paul Scherrer Institut, CH-5232 Villigen, Switzerland.